Cliodynamics: The Journal of Quantitative History and Cultural Evolution

Modeling the Large-Scale Demographic Changes of the Old World

James Bennett
University of Washington

I investigate the predictive ability of a simple demographic model for agrarian empires in several Old World geographies between 1500 BCE and 1500 CE. I estimate and bound key model parameters from two historical datasets. I find that quasi-uniform carrying capacities and two net birth rates suffice to predict most Old World agrarian empire demographics in this period. This analysis suggests that a doubling of agricultural intensification occurred throughout most of the Old World circa 1000 CE.

Introduction

The impact of changing demography on polities has long been a staple of historical analysis. The observations of Malthus (1798) led to subsequent criticism and improvements (Ricardo, 1821), including, recently, demographic-structural theory (Goldstone, 1991).

In spite of the uncertainty of many historical population estimates (see Kaplan and Krumhardt, 2008 for a review), such models may be sufficiently accurate at large scales (e.g., 100 years, 1 million km^2) to test the predictions of current scientific models of historical processes. Having a model that makes plausible historical demographic predictions would be a useful component for both driving and evaluating models of historical processes.

Traditionally, demographic models have focused on predicting age and sexual cohort distribution over relatively short periods of time given different policy or mortality events (see Coale and Trussell, 1996). These models are typically applied to contemporary scenarios, predicting, for example, demographic transitions during industrialization. These models require details typically unavailable in the historical record that may not even be applicable to certain historical polities.

Here, I develop a simple, agent-based demographic model for agrarian states that makes gross population predictions plausible when tested against actual historical empire data in the Old World between 1500 BCE–1500 CE. After reviewing the historical data and describing the model, I investigate its behavior in several geographic subsets and compare its predictions against historical

Corresponding author's e-mail: jsb11@u.washington.edu

Citation: Bennett, James. 2015. Modeling the Large-Scale Demographic Changes of the Old World. *Cliodynamics* 6: 57–76.

population estimates. The model itself makes certain predictions about underlying processes and, thus, can be employed to evaluate various agent-based models of state formation in the Old World. These will be investigated in future papers.

The Historical Data

I developed and evaluated my model by employing two data sources. The first dataset, referred to here as the TCTG13 dataset, was developed by Turchin et al. (2013) to evaluate their model of ultra-sociality development in the Old World. One part of the dataset describes the Afro-Eurasian continent as a gridded landscape of regions, encoding mean elevation and predominant 'biome type': desert, steppe, or agricultural. More fully described in their Supplemental Data, regions were assumed to occupy 10 thousand km^2 (100^2 km^2). Each TCTG13 land region is connected to its immediate cardinal neighbors if they exist; certain regions are marked as littoral if any of their neighbors are an ocean or a sea.

The original TCTG13 dataset was supplemented by latitude and longitude coordinates for each region, rather than the ordinal values assigned for the study. This allowed the computation of the actual area of each region, which varies by (the cosine of) latitude, with a border size of 111.32 km per degree at the equator. As it happens, the TCTG13 regions are, in fact, rectangular, stretching about 2 degrees of longitude and 1 degree of latitude and occupying about 25 thousand km^2 at the equator. In addition, several minor biome types and littoral encoding errors were also identified and corrected, none of which, like the area difference, would have had any impact on the reported results of Turchin et al. but are important to the results below.

The TCTG13 dataset also encodes the regional locations of all large-scale, centralized macro-states ('empires') present at each century between 1500 BCE and 1500 CE (the Old World). Each encoded empire occupied at least 10 TCTG13 regions (100 thousand km^2, roughly the size of the contemporary Czech Republic or the historic Duchy of Burgundy).

The second dataset encodes the spatially and temporally resolved population estimates of Kaplan and Krumhardt (2008), referred to as KK10. This dataset contains yearly population estimates between 6050 BCE and 1850 CE. Based, in turn, on several well-known sources of historical population data (e.g., McEvedy and Jones, 1978), the population dataset is organized by modern, worldwide 'territories' (e.g., Paraguay, Minnesota, etc.). A separate territorial definition dataset, also supplied by Kaplan, provides latitude and longitude for each modern territory region, resolved to .08 degrees. Combined, the KK10 datasets permitted per-century estimates of population for selected rectangular subset landscapes of the TCTG13 Old World data, which I employed to evaluate and improve the model. Where the KK10 territories overlapped a TCTG13 subset region by less

than 10 percent, their population estimates were discarded. TCTG13 subsets were chosen to avoid large population inconsistencies.

In particular, I focused on three subset landscapes in addition to the entire Old World (Figure 1): the European plus Middle Eastern theater ('Europe+ME'), the Indian subcontinent plus Middle Eastern region ('India+ME'), and China plus Southeast Asia ('Asia'). Figure 1 indicates these subset region locations as well as the distribution of all agricultural regions. Each of these study regions was chosen because these theaters developed relatively independently of one another, at least for the first millennium. Furthermore, together, these landscapes account for over 90 percent of the total population and empires of the Old World. Importantly, however, their spatial and population growth dynamics are very different, apparently because of their very different geographies (Diamond, 1997). (The northern steppe and African regions are omitted as regions of interest because they contributed very little to the agrarian empire and world population record in this time period.)

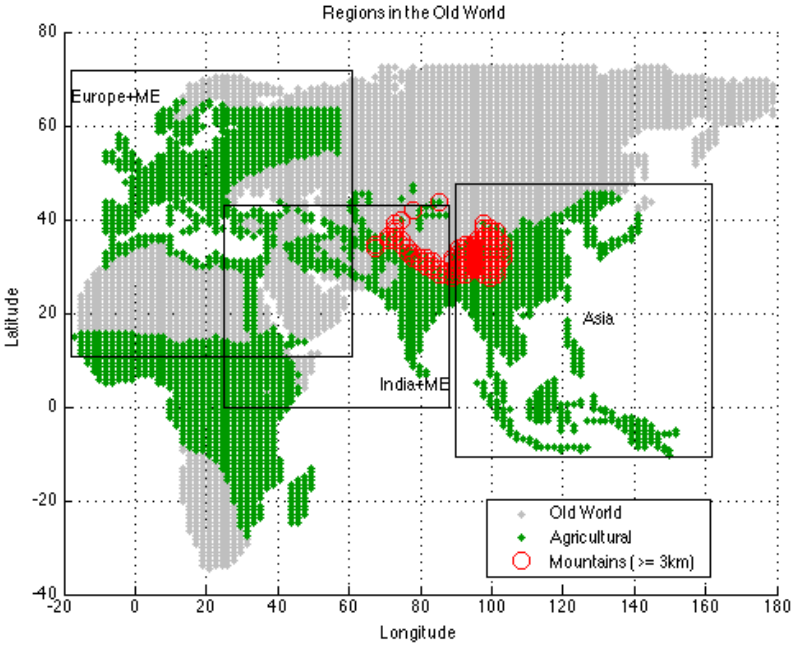

Figure 1. Agricultural regions in the Old World and the study subset landscapes.

Figure 2 plots the increase of total area occupied by historical empires during the study period using a linear spatial interpolation method described below and

applied to the TCTG13 data. The TCTG13 dataset encodes the location of empires that were primarily agrarian but also includes nomadic pastoralist empires. There are roughly two major agrarian expansion periods (600 BCE–100 CE and 700 CE–1300 CE) between flanking periods of relatively little expansion. The waves of large-scale, nomadic empires that pestered the agrarian empires after 300 BCE are also clearly visible. An accompanying movie (see Supplemental Data) animates the location, extent, rise, and fall of the empires encoded in the TCTG13 dataset.

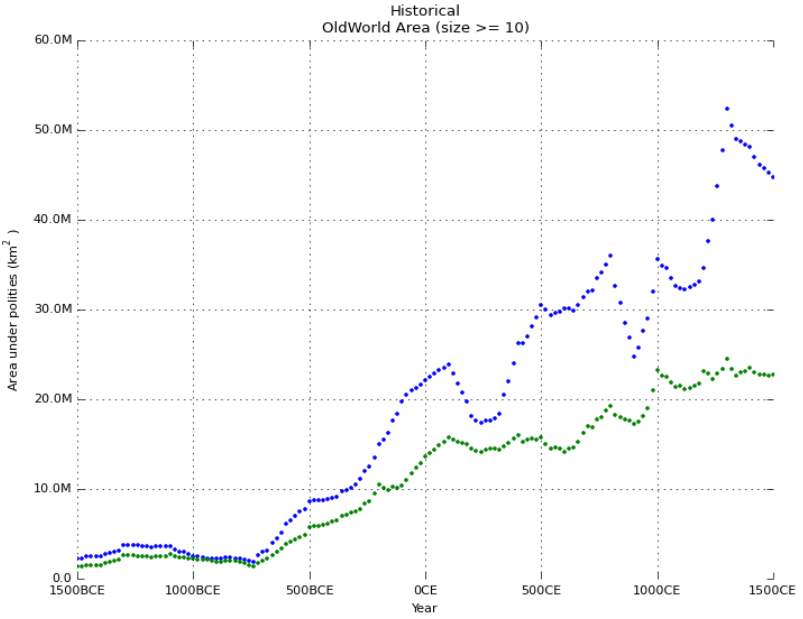

Figure 2. Area under agrarian (green) and all (blue) empires, as interpolated from the TCTG13 dataset of Turchin et al. (2013).

Figure 3 shows the corresponding total population of the Old World to the nearest century from the KK10 dataset. A weakly quadratic rise from 70 million to 390 million occurs in this period, with some major episodes of plague and famine clearly present in the record, notably the Justinian pandemic and Chinese famines and plagues beginning around 200 CE and the Black Death in the mid-fourteenth century.

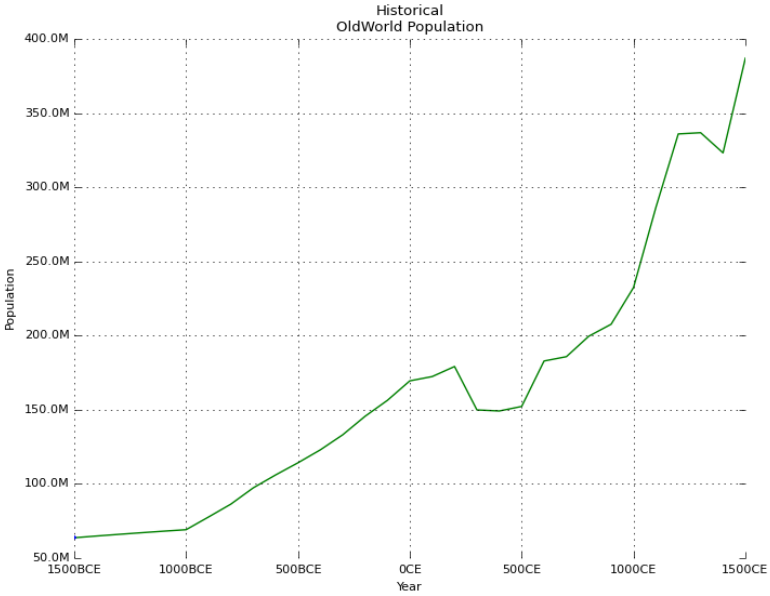

Figure 3. Old World population estimates from the KK10 dataset of Kaplan and Krumhardt (2008).

The Demographic Model

The core of the demographic model is simple. Each agricultural region, *r*, in the modeled landscape is characterized by a current population (P_r; units: people) and a carrying capacity (K_r; units: people). With the exception of nomadic empires, non-agricultural regions (e.g., steppes and desert) are assumed to have negligible populations and carrying capacities.

Each agrarian region can be occupied by one of two *types* of polities: a single-region 'hinterland' polity or a multi-region 'empire' polity. Each polity type has an associated net birth rate (β_h, β_e; unit: percent/yr) and an assumed 'natural' supportable population density (ρ_h, ρ_e; unit: people/km^2), from which carrying capacity is derived based on the area of the region. A multi-region polity is assumed to require greater administrative organization and supply greater stability and investment in infrastructure at scale and, thus, will enjoy both a larger population density and net birth rate over a single-region hinterland. In particular, Pinker (2011) has argued that the rise of large states and their internal mechanisms for quelling violence between neighbors (police, courts) lead to a

substantial decrease in mortality. Below, I estimate the relative benefit of polity type from the historical data.

As modeled history unfolds, the polity type of a region may change as, for example, hinterland is annexed into empires and empires collapse back to hinterland. When a region changes its polity type, the corresponding population density is employed to compute the new carrying capacity, and the new net birth rate is used to compute subsequent changes to the existing population. Thus, the model integrates regional population responses to imposed polity changes.

There are four such transitions possible in the model. First, an existing empire may annex an arable hinterland region; this empire expansion ('extensification') increases the carrying capacity and net birth rate of the annexed region. Conversely, an empire may collapse, and some of its regions might revert to hinterland, decreasing the regional carrying capacity and net birth rate of the lost regions. One empire might annex the region of another empire, but because the *type* of polity does not change, neither carrying capacity nor net birth rate changes. Finally, an empire might arise from hinterland regions. In this case, all the empire regions increase carrying capacity and net birth rate.

Following Ricardo (1821), Turchin (2002), and many others, I model population growth in a region as logistic, reflecting the declining ability of residual carrying capacity to support additional population:

$$\dot{P}_r = \beta(\tau_r)\left(1 - \frac{P_r}{K_r}\right)P_r\,, \tag{1}$$

$$K_r = \rho(\tau_r)\,A_r, \tag{2}$$

where $\beta(\tau_r)$ is the net birth rate and $\rho(\tau_r)$ is the population density associated with the polity type τ_r in region r with area A_r. The term $1-(P_r/K_r)$ reflects the residual regional *opportunity* remaining for additional population growth, a fraction of residual carrying capacity. Values for β reflect the typical net birth rates at low actual population densities for the two types of polities.

Estimating Historical Population Densities and Net Birth Rates

I employed the historical data to estimate values for the two population densities and their corresponding net birth rates. To estimate the empire population density and net birth rate values, I sought historical regions where empires arose from essentially a hinterland state, whose subsequent demographics are reasonably well-known and yet were relatively unmolested by rebellions, wars, famines, or plagues, and that apparently came close to saturating their available carrying capacity before finally succumbing to one of those four horsemen.

One such polity is medieval England after William the Conqueror's invasion in 1066 CE. As an island, William's England had been relatively isolated from other Continental adventures for several hundred years. Although the debate over medieval British population figures is not resolved, population estimates based on extensive sources, such as the Domesday Book and various ecclesiastical records (Campbell, 2000), make estimating population sizes and land and yields under cultivation, for my crude purpose, straightforward.

Campbell (2000, Chapter 8) argues that the population grew from 1 million to a peak of 3 million between 1150 CE and 1312 CE, when the Great Famine checked population growth, followed by a population collapse during the Black Death in 1348 CE. These population values are close to the values in the KK10 dataset of 1.7 million and 3.47 million, respectively, but differ from those of Hallam as quoted by Postan in Turchin and Nefedov (2009), of 3 million and 6 million, respectively. Below, I employ the estimates of Campbell (2000).

During this period, the area occupied by the Norman English was smaller than the present United Kingdom, essentially excluding Ireland and Scotland, and was concentrated in the productive Midlands. At its peak, I assume it occupied approximately 148 thousand km^2 of arable land (12 TCTG13 regions at 53°N).

The decades following William's conquest and death were unstable because his sons Robert and William, then Henry, contested for control of Normandy and England. I thus assume England was not a consolidated, stable polity until roughly 1150 CE and treat it as a set of hinterland regions at that time for the purposes of these estimates. I also assume that it then consolidated into a multi-region empire and finally neared carrying capacity saturation in 1300 CE, after a period of 150 years. It is unlikely, however, that either polity type ever saturates its carrying capacity (Turchin, 2003). Further, historical studies (Brenner, 1976) suggest that the population (typically, the elites) consumes some fraction of the carrying capacity non-productively. I assume that 'tax' to be 20 percent; applying it to Campbell's (2000) population figures implies a starting hinterland potential population density ρ_h of approximately 8 people/km^2 in 1150CE and a final empire potential density ρ_e of approximately 24 people/km^2. The ratio of these two values, 3:1 (or 2:1, if using the KK10 or Hallan population estimates), is a direct measure of the improvement a stable agrarian empire can provide relative to hinterland.

To estimate the net birth rate under an empire, I solve Equation 1 for β_e. After some integration and rearrangement, in general:

$$\beta = \lambda_\beta(P_0, P, K, t) = \frac{\log\left(\left(\frac{P}{P_0}\right)\left(\frac{K-P_0}{K-P}\right)\right)}{t}, \quad (3)$$

where t is the time it takes to grow a starting population P_0 to a final population P, given an estimated carry capacity, K. Solving λ_β(1M, 3M, 1.2×3M, 150) yields a net empire birth rate of 1.71 percent/year, a plausible net birth rate for a largely monogamous population at very low densities. Recall that, according to Equation 1, the *effective* net birth rate depends on the residual opportunity in addition to this base rate. As polities mature, their larger populations reduce the residual opportunity, yielding effective regional birth rates that are fractions of this base rate.

Finally, I estimated a hinterland net birth rate in a similar fashion to the medieval case. I searched for regions and periods where *no* empires were present in the TCTG13 dataset and yet the historical (growing) population estimates of KK10 were plausible and not obviously interpolated. I found 71 such examples (e.g., most of modern Europe prior to 400 BCE, sub-Saharan Africa before 0 CE, Southeast Asia before 100 CE). I assume they were quite near their (lower, non-empire) carrying capacity and, thus, Equation 3 predicts a much smaller net birth rate. These examples consistently suggest that the hinterland net birth rate is around one-tenth of that under empire, approximately 0.2 percent/year.

Population Collapse

Three other effects need to be accounted for in the model.

Given small values of β, Equation 1 ensures that P approaches K rather gently from below, depending on the opportunity term. In cases where a hinterland region is annexed by an empire, the population grows rapidly, reflecting both the improved birth rate and larger opportunity due to increased potential carrying capacity. However, in cases where the population suddenly exceeds the available carrying capacity (for example, when an empire region falls back to hinterland and the advantage of empire evaporates in chaos and local famine), the opportunity term is negative and the region's population will decline toward the new lower circumstances but at effectively the negative hinterland net birth rate.

Empirically, I observed that, in spite of an initially high negative opportunity, the effective rate of decline was too gentle because of the low value of β_h. Thus, in the case of negative opportunity, I model the typically precipitous population crash as an immediate fall—indeed, an overshoot—of population below the new available K by setting the population to a fraction, δ, of K.

$$\dot{P}_r = \begin{cases} -(P_r - \delta K_r) \text{ if } \left(1 - \frac{P_r}{K_r}\right) < 0 \\ \beta(\tau_r)\left(1 - \frac{P_r}{K_r}\right) P_r \text{ otherwise} \end{cases} . \tag{1a}$$

I was unable to derive a death fraction, δ, directly from the historical data but observed empirically that a value of 80 percent adjusted the population below

available carrying capacity rather smartly and appeared to match the historic population data. This value of δ was adopted throughout all the simulations described in this paper.

Migration

Consider a large empire such as the Shang that arose in 1500 BCE, tripled its territory in 1300 BCE by annexing surrounding hinterland, and then collapsed in 1100 BCE. In this case, the early 'core' regions of the empire will have become more saturated with people yielding less opportunity for growth compared to the later, 'peripheral,' frontier regions. We should expect at least some population migration to occur as people move to enjoy the relatively larger opportunities in the frontier regions after their acquisition (McNeill, 1984).

I implemented a simple *within-polity* migration scheme that moves population away from more saturated regions and toward lands of higher opportunity. Migration occurs by redistributing a constant fraction, μ, of the existing population at each simulation time step. The migrating population is taken from all the polity's regions in proportion to their population and is then redistributed proportionally to the opportunity remaining in each region. As the regional populations become uniform throughout the polity, the opportunity gradient decreases and the number of people redistributed tends to zero.

A very high migration fraction suggests a restless and, until modern times perhaps, unrealistic society. For example, if the migration fraction was the maximum 100 percent, each time step would ensure that the entire population was uniformly distributed immediately. Any smaller fraction implies that it takes longer to achieve uniform population distribution because there will always be some residual unexploited opportunity. Because the redistribution of people has the effect of temporarily increasing the regional opportunity (since people move away from saturated regions), Equation 1 tells us to expect higher population growth rates and, as a consequence and depending on the longevity of occupying empires, the resultant population will be higher. In the Supplemental Data, I show that small migration fractions have a modest but discernable positive impact on the total predicted population over three millennia.

The migration fraction represents the portion of the population willing (or forced) to move at least one region; this distance is roughly 100 km and sometimes many times that for larger empires. Except perhaps for armies, this was a large, even daunting, distance to travel routinely in the modeled time period, so we should not expect a very high value for μ. Indeed, I assume that most people would prefer to remain near their birthplace and their local extended families. In all the simulations investigated here, I employ a μ of 0.2 percent, roughly 10 percent of our assumed empire net birth rate. All moves happen within a time step, regardless of distance.

Initialization

At the beginning of the simulation the model must make an assumption about the how the *observed* population from KK10 is distributed amongst the initial empire and hinterland polities. To do this the model divides the initial observed population KK10(t_0) proportionally amongst the agricultural regions depending on their initial polity state, whether hinterland or empire, and according to the ratio of expected population densities and the areas of those regions. It first computes an effective actual hinterland population density ρ_{h0} and then scales it by the expected population density ratio for empire states.

(4) $$\varphi = \frac{\rho_e}{\rho_h}$$

(5) $$\rho_{h_0} = \frac{KK10(t_o)}{(\varphi \sum_{empires} A_r + \sum_{hinterland} A_r)}$$

It then sets all hinterland P_r to $\rho_{h0}A_r$ and all empire P_r to $\varphi\rho_{h0}A_r$. Thus, all empires (and hinterland) are treated as having a relatively equal starting state, an admittedly poor assumption. However, it made little difference in practice for this model because the major driver of population dynamics is the waxing and waning of historical empire polities, which quickly dominate whatever starting variation might have been present.

Investigations and Results

I tested the model by employing the actual historical empire transitions supplied by the TCTG13 dataset each century in our study period. To permit more resolved temporal population estimates, I assumed that the historic regional polity assignments, whether empire or hinterland, transformed 'linearly' between adjacent centuries. In particular, for each new century, the model determines the set of regions whose polity-type assignment would change and arranges to stochastically flip these regions' polities at a computed rate, which depended on the number of changes and time-step resolution of the simulation, such that all changes were accomplished within the ensuing century. This spatial-temporal interpolation 'dissolved' one century directly into another and permitted a smoother estimation of the modeled population. In all simulations in this paper, the time step was two years.

The two panels of Figure 4 show the results of the model simulation in the Old World. The left panel shows the Old World agrarian (green) and total (blue) empire area data (here repeating data from Figure 2). The right panel shows the model predictions every 20 years (blue marks) for different assumptions about ρ_h and ρ_e in the Old World, compared with the corresponding KK10 population data

(green line, here repeating Figure 3). The initialization calculation (Equation 5) ensures the model prediction matches the initial observed population in all cases. The top-most blue line, which significantly overshoots the middle millennial population, is based on the population densities derived above from medieval England and applied anachronistically to the historical record. In hindsight, this model failure is not surprising: We should not necessarily expect ancient Egypt, for example, to match the productivity of medieval England two millennia later. After all, the vast majority of the Old World that eventually became arable was under some form of forest or otherwise unworked in 1500 BCE (Ellis, et al. 2014, McNeill, 1984) and was unlikely to support even the medieval hinterland density calculated above.

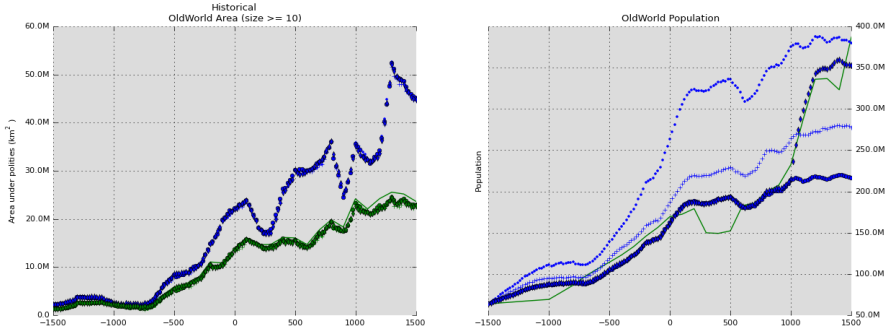

Figure 4. Area and population predictions for the Old World under different intensification schedules. A) Area under agrarian (green) and all (blue) empires. Solid green line represents historical agrarian data from the TCTG13 dataset of Turchin et al. (2013); points represent interpolation every 20 years. B) Population predictions from the demographic model between 1500 BCE–1500 CE. Solid green line represents historical data from KK10 dataset of Kaplan and Krumhardt (2013); points represent predictions every 20 years. See main text for marker descriptions.

Empirical investigation suggested that the early population density values should be about half of the medieval values (ρ_e = 12 people/km^2, ρ_h = 4 people/km^2, preserving the empire/hinterland ratio). The middle prediction (Figure 4B, blue crosses) shows the result of this assumption. It tracks the population well in the first millennia before substantially overshooting during the period of the Roman and Han Empires, yet ends under-predicting the population after 1000 CE.

Investigation of the model's response with these alternative starting density values in the different regional landscapes indicated two effects at work. First, it was clear that not all regions enjoyed the same early productivity as others.

Notably, the Mesopotamian and sub-Saharan African regions required initial densities that are two-thirds of our alternative starting values. More importantly, however, the population densities needed to increase at some point to match the doubled values estimated from medieval England above. This rise appeared to occur nearly simultaneously in most arable regions around 1000 CE.

The overall population prediction for the Old World based on these combined assumptions is shown as the lower blue lines in Figure 4B, which show separately the impact of regional variation and the doubling in carrying capacity in 1000 CE. Because the model does not deal with famine and plague, it misses the large-scale drops in population. However, a case could be made that if the Justinian plagues had not occurred, the population trend during this period might plausibly have followed the predictions of the model. Without the doubling assumption, the population prediction diverges at least around 1000 CE, although it might have occurred earlier but was masked by the earlier famines and plagues. When the carrying capacities are doubled in 1000 CE, the predicted population more closely matches the observed Old World population.

Intensification

I implemented productivity assumptions by modifying Equation 2 to reflect a multiplicative agricultural 'intensification' term that was exogenously applied regionally and temporally according to different schedules, resulting in

(2a) $$K_r = \rho(\tau_r)\, I_r(t)\, A_r,$$

where t is the year of the simulation. By default, the intensification term, $I_r(t)$, is 1 everywhere and, as employed in this model, is *not* dependent on polity type. Instead, I employ $I_r(t)$ to capture natural productivity variation by regional biome type or elevation and also to reflect common social and technological improvements assumed available to all polities.

The actual exogenous intensification schedule employed by the model is a bit more complicated. The intensification of European, Asian, Indian and possibly African theaters, which constitutes the majority of the Old World, all apparently doubled around 1000 CE. However, following Turchin et al. (2013), some high latitude regions, especially in northeastern Europe, northern Britain, Japan and northeastern China, initially had poor yields but became partially productive around 300 CE. In 700 CE, an additional zone in the Rus also became partially productive. However, these two regions did not apparently double their intensification in 1000 CE. I also assumed that mountainous regions higher than 3 km were never agriculturally productive. Figures 5A and 5B summarize the intensification location and schedule employed in all subsequent simulations.

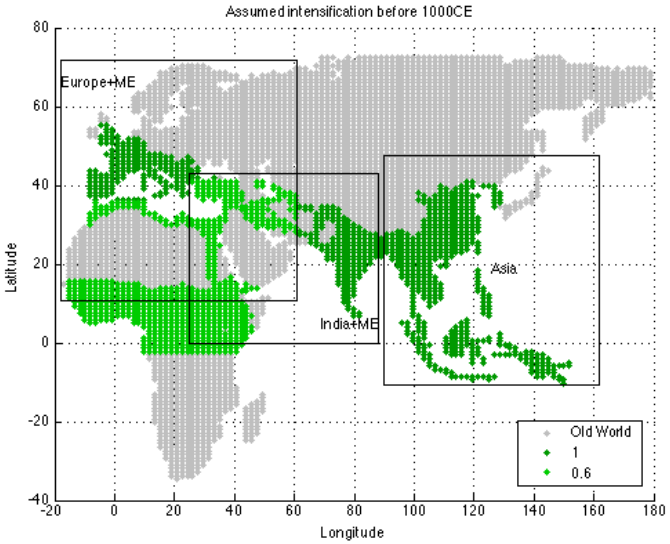

Figure 5A. Early intensification schedule

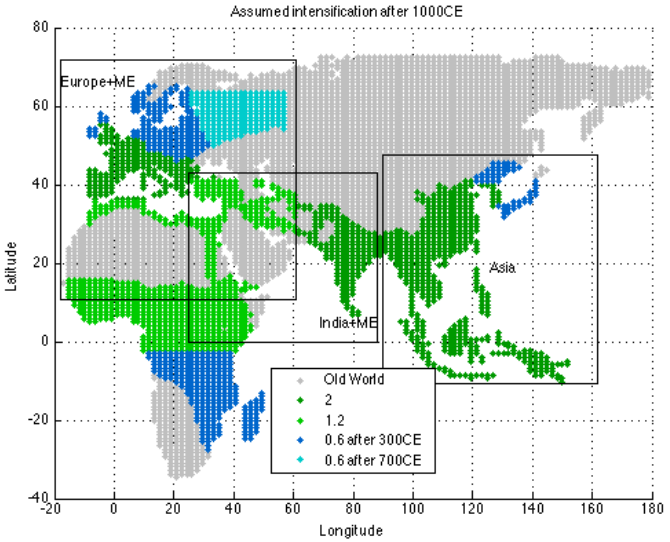

Figure 5B. Late intensification schedule

Population predictions in subsequent figures are based solely on this final intensification schedule.

Table 1 summarizes the final values of the demographic model's parameters applied to the Old World. The intensification schedule described above then scales the population density parameters temporally and regionally.

Table 1. Demographic model parameters for the Old World

Parameter	Value
Hinterland population density, ρ_h	4 people/km^2
Empire population density, ρ_e	12 people/km^2
Hinterland net birth rate, β_h	0.2 percent/year
Empire net birth rate, β_e	1.71 percent/year
Non-productive 'tax' on carrying capacity	20 percent
Within-polity migration fraction, μ	0.2 percent/year
Collapse fraction, δ	80 percent

Asia

Reviewing the demographic model's performance in the different subset landscapes is revealing. I turn first to the predictions in the Asian landscape, whose population dynamics are dominated by the various Chinese dynasties. The model results are shown in the two panels of Figure 6. As in Figure 4, the left panel shows the areas under empire for this theater and the right panel shows the KK10 observed (green) and model predicted (blue) populations, with and without intensification doubling in 1000 CE. Initial empire occupation was essentially stable and relatively small during the first millennia of our period, corresponding to the Shang through the Spring and Autumn period of the Chou. Around 300 BCE there was a significant increase in occupied agricultural land during the Warring States period and then, around 200 BCE, a large increase in the nomadic empires (the Hun) during the early part of the Han. Agrarian empire area then increased roughly linearly, accompanied by periodic bouts of nomadic empires' expansion and contraction. The period ends as the Ming dynasty begins its collapse.

The sparse population data from KK10 are clearly interpolated in the beginning of the record but, after 0 CE, reflect improved census data and show the impact of massive famines and plagues at roughly the same time as the Justinian plagues in Europe (which likely originate from the same steppe source). This is followed by a partial recovery and, then, substantial upturn in population after 1000 CE. The population dip around 1200 CE is due to the chaos of the great Mongol war, the loss of the Chin in the north, and the Mongol advance nearly to Japan.

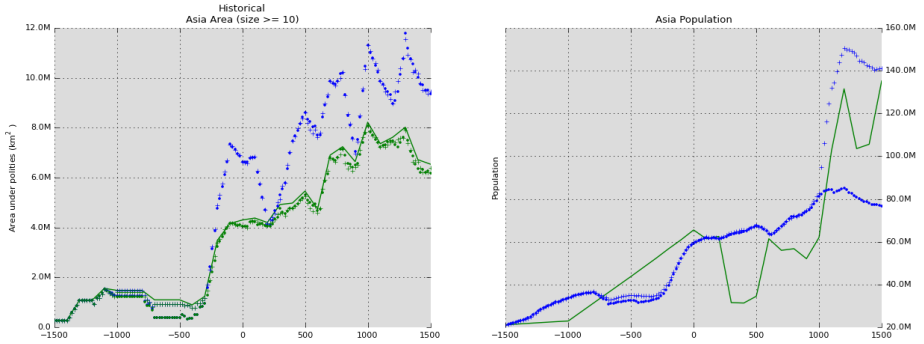

Figure 6. Area and population predictions for Asia, incorporating intensification in the demographic model. A) Area under agrarian (green) and all (blue) empires. Solid green line represents historical agrarian data from the TCTG13 dataset of Turchin et al. (2013); points represent interpolation every 20 years. B) Population predictions from the demographic model between 1500 BCE–1500 CE. Solid green line represents historical data from KK10 dataset of Kaplan and Krumhardt (2013); points represent predictions every 20 years. See main text for marker descriptions.

Although the constant intensification population model (Figure 5A) follows the trend of population data well (excluding the famines after 0 CE), it somewhat underestimates the population until 1000 CE, when again it completely fails to predict a rapid increase in population. However, doubling the intensification in 1000 CE permits a plausible population prediction. Critically, at this time, there is no corresponding increase in area under empire; indeed, the area is stable or decreasing during this period, strongly suggesting that the carrying capacity increase was due to increased intensification practices rather than to extensification by annexation.

Europe and the Middle East

The Europe+ME zone shows, in Figure 7A, two early pulses of agrarian empire area increase and a somewhat constant area under nomadic rule until 500 CE, when substantial nomadic expansion occurs. The agrarian increase in 500 BCE is due largely to Persia, the increase in 0 CE is due to Rome, and the increase in 1000 CE corresponds to the initial rise in the classic western European proto-states (France, England, Spain, Germany, etc.).

The historical population data (Figure 7B, green line) again track the increase of agrarian land under empire, and, in particular, show a large increase during the Roman occupation of Europe. Following 200 CE, the population declines with the onset of the Justinian plagues and the collapse of the empire but rapid rises

during the middle and late medieval period. The predictions of the constant intensification model correspond well to the data, even capturing some of the population decline after the fall of the Roman Empire but then, once again, missing the substantial historical increase after 1000 CE. Applying the doubling intensification assumption allows the predicted population to better match that portion of the record.

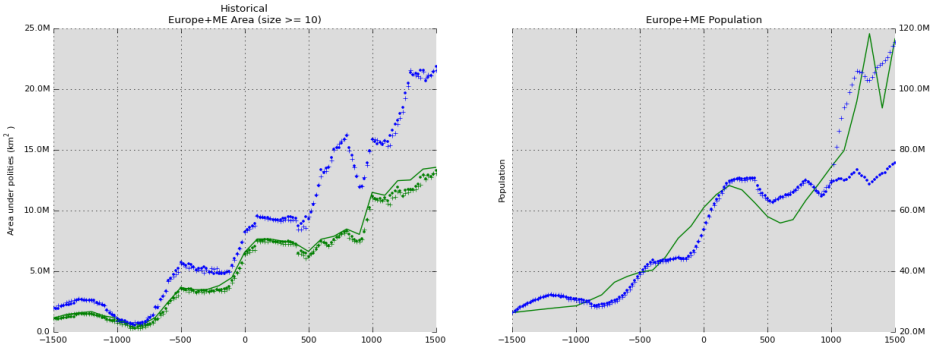

Figure 7. Area and population predictions for Europe and the Middle East, incorporating intensification in the demographic model. A) Area under agrarian (green) and all (blue) empires. Solid green line represents historical agrarian data from the TCTG13 dataset of Turchin et al. (2013); points represent interpolation every 20 years. B) Population predictions from the demographic model between 1500 BCE–1500 CE. Solid green line represents historical data from KK10 dataset of Kaplan and Krumhardt (2013); points represent predictions every 20 years. See main text for marker descriptions.

India and the Middle East

Finally, the Indian theater shows a similarly slow acquisition of agrarian territories during the 700 years after the collapse of the Indus Valley civilization in 1500 BCE (Figure 8). This is followed by a rapid increase of agrarian land around 500 BCE and is accompanied, as in the Asian zone, by a significant rise in nomadic empires. The saw-tooth nature of both agrarian and nomadic empire area reflects the nearly synchronous rise and fall of several Indian and nomadic empires. After 200 BCE, the agrarian empires saturated the available land in the zone, repeatedly collapsing and reforming.

In spite of these dramatic oscillations, the KK10 population data show a largely linear or weakly quadratic increase throughout the three millennia. There are no indications of additional large-scale population collapses due to famines and plagues as in the other zones, though they undoubtedly occurred. Although

one might question the population data (or its interpolation), if it is taken at face value, the population model does well enough for the first millennia and a half, then substantially underestimates the population for the remaining period. Because the arable land is saturated early, the population also saturates as the residual opportunity dwindles to zero. The model's final prediction, even after applying the doubling of intensification, is a factor of 2.3 below the historical data. However, reviewing the contributing data employed by Krumhardt (2014) to estimate the Indian population, the data of Biraben (1979; Krumhardt's Fig 2 [h], yellow line) has a qualitative shape that resembles the model's prediction, even if the data values are overall higher. If the model's assumptions are as plausible as the original data sources for India, its output could stand as a prediction that further investigation might bear out.

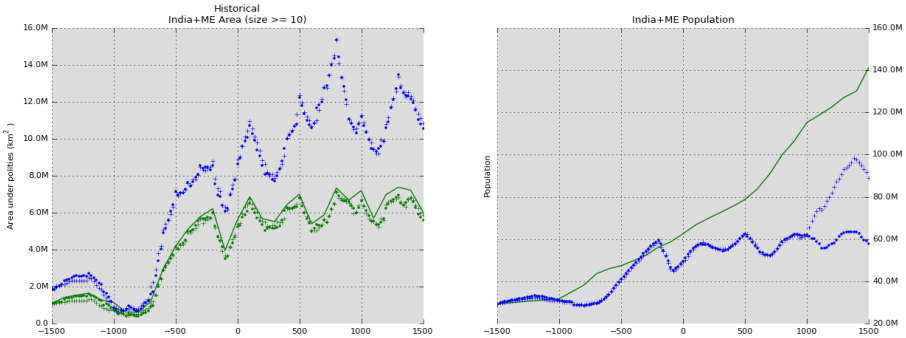

Figure 8. Area and population predictions for India and the Middle East, incorporating intensification in the demographic model. A) Area under agrarian (green) and all (blue) empires. Solid green line represents historical agrarian data from the TCTG13 dataset of Turchin et al. (2013); points represent interpolation every 20 years. B) Population predictions from the demographic model between 1500 BCE–1500 CE. Solid green line represents historical data from KK10 dataset of Kaplan and Krumhardt (2013); points represent predictions every 20 years. See main text for marker descriptions.

Discussion

The model's main assumption is that changing polity type from small-scale hinterland to a larger-scale empire supports trebling population density in the Old World. The results reported here depend, of course, on the temporal assignment of regions by polity type. The Turchin et al. (2013) dataset encoded only fairly large polities as empires (at least 10 TCTG13 regions) every century, missing some well known but smaller polities such as ancient Greece. As additional polities of intermediate size (and perhaps different types reflecting

different management schemes) are encoded (Turchin, 2014), this simple step-function assumption may require refinement.

The model employs a quite coarse intensification schedule. The population record of first two millennia after 1500 BCE suggests no apparent major intensification change. Further, when the substantial changes do occur, late in the record (300 CE, 700 CE, and 1000 CE), they are persistent: Each of these changes involves hundreds of TCTG13 regions (at least 2 million km^2) that then last for centuries. As more detailed data on plant distributions and their yields, domesticated animal populations, and agricultural technology become available (Turchin, 2014), increasingly refined intensification schedules may be required and perhaps even made endogenous by various models. Overall, however, the three millennia modeled here appear to be a time of relative stasis in terms of agricultural innovation, when people were more engaged in occupying additional arable land than improving it.

The intensification doubling in 1000 CE is likely due to many different technical and social innovations adapted to the different land and crop types and political arrangements in each region rather than a single common technological innovation. In Asia, for example, rice varieties were improved during the Song dynasty and rice itself is a crop that can be increasingly intensified with communal labor maintaining the terracing and hydraulics required to supply nutrients and monitoring for pests (Geertz, 1963). Wheat and oats in the European theater benefited from three-crop rotation schemes and improved plowing technology (Campbell, 2000). Indeed, intensification continued after 1500 CE, again roughly doubling medieval wheat yields from approximately 6 bushels per acre in 1300 CE to approximately 15 bushels per acre by 1850 CE. Intensification then remained unchanged until 1945 CE, when the broad availability of chemical fertilizers and subsequent development of improved crop strains increased yields by a factor of 6 to over 90 bushels per acre presently. Rice, the other major staple grain, followed a similar trajectory.

Regardless of how it was achieved (with the possible exception of India), the medieval doubling of Old World-wide carrying capacity occurred nearly synchronously with the saturation of all the Old World arable land by agrarian empires. Because expansion of agriculture had effectively ceased and unoccupied arable land grew scarce, the pressure to find innovative ways to intensify the existing arable land to support the growing population would have been intense (Kremer, 1993; Boserup, 1981).

Famine and plague were not incorporated into the present model, although for the historical record investigated here, they could have been added easily as exogenous, temporary decreases in intensification and population, respectively, for certain regions. Future models of polity rise and fall may predict when and where such events might occur, especially if they are induced, for example, by

poor management of crops, regional climate changes, or increased population densities in urban environments (McNeill, 1984). A similar future awaits modeling the exogenous intensification increases employed by the present model when investigating mechanistic ideas of societal innovation and technology adoption.

In any case, the demographic model presented here suggests that, however future imperiogenesis models predict the rise, expansion, and collapse of empires in the Old World, to the extent they match the rate and location of historical agrarian territorial gains, plausible population predictions at this large scale follow from a few surprisingly simple demographic assumptions.

Acknowledgements

I thank Peter Turchin and Tom Currie for their patience, encouragement, illuminating discussions, and for sharing and clarifying the TCTG13 dataset. I thank Jed Kaplan for sharing his KK10 world population dataset. I thank Fritz Stahr and Stan Lanning for comments on early drafts of this paper.

References

Boserup, Ester. 1981. Population and Technological Change: A Study of Long Term Trends. University of Chicago Press, Chicago.

Brenner, Robert. 1976. Agrarian Class Structure and Economic Development in Pre-Industrial Europe. Past & Present 70:30-75.

Campbell, Bruce M. S. 2000. English seigniorial agriculture 1250-1450. Cambridge, Cambridge University Press.

Coale, Ansely and James Trussell. 1996. The Development and Use of Demographic Models. Populations Studies. 50(3): 469-484.

Diamond, Jared. 1997. Guns, Germs, and Steel: The Fates of Human Societies. W. W. Norton, New York.

Ellis, Erle C., Jed O. Kaplan, Dorian Q. Fuller, Steve Vavrusd, Kees Klein Goldewijke, and Peter H. Verburgf. 2013. Used planet: A global history. PNAS, 110: 7978–7985.

Geertz, Clifford. 1963. Agricultural Involution: The Process of Ecological Change in Indonesia. University of California Press, Berkeley, CA.

Goldstone, Jack A. 1991. Revolution and rebellion in the early modern world. University of California Press, Berkeley

Kaplan, Jed O., Kristen M. Krumhardt, Erle C. Ellis, William F. Ruddiman, Carsten Lemmen and Kees Klein Goldewijk. 2011. Holocene carbon emissions as a result of anthropogenic land cover change. The Holocene 21(5): 775-791.

Kremer, Michael, 1993. Population Growth and Technological Change One Million B.C.to 1990. Quarterly Journal of Economics. 108(3): 681-716.

Krumhardt, Kristen M. 2010. ARVE Technical Report #3: Methodology for world-wide population estimates: 1000 BC to 1850. École Polytechnique Fédérale de Lausanne, Dept. of Environmental Engineering, ARVE Research Group, http://arve.epfl.ch/technical_reports/ARVE_tech_report3_pop_methods.pdf.

Malthus, Thomas. 1798. An essay on the principle of population, in A Commentary on Malthus' 1798 Essay on the Principle of Population as Social Theory, edited by F. Elwell, pp. 127–294, Mellen Press, Lewiston, commentary printed 2001.

McEvedy, C. and R. Jones, 1978. Atlas of World Population History. Penguin Books Ltd., London.

McNeill, William H. 1984. Human Migration in Historical Perspective. Population and Development Review 10(1) pp.1-18.

Nefedov, Sergey A. 2013, Modeling Malthusian Dynamics in Pre-Industrial Societies, Cliodynamics, 4(2)

Pinker, Steven. 2011. The Better Angels of Our Nature: Why Violence Has Declined. Viking Press.

Ricardo, David. 1821. Principles of political economy, third ed., John Murray, London.

Turchin, Peter. 2003. Historical Dynamics: Why States Rise and Fall. Princeton University Press.

Turchin, Peter 2005. Dynamical Feedbacks between Population Growth and Sociopolitical Instability in Agrarian States. Structure and Dynamics 1(1): Article 3.

Turchin, Peter and Sergey Nefedov. 2009. Secular Cycles. Princeton University Press.

Turchin, Peter, Thomas E. Currie, Edward A. L. Turner, and Sergei Gavrilets. 2013. War, Space, and the Evolution of Old World Complex Societies. PNAS, 110: 16384–16389.

Turchin, Peter. 2014. The SESHAT Databank Project: the 2014 Report. Cliodynamics, 5(1).